Outstanding Magnetic Properties of Nematic Suspensions of Goethite (α-FeOOH) Nanorods

B. J. Lemaire,[1] P. Davidson,[1,*] J. Ferré,[1] J. P. Jamet,[1] P. Panine,[2] I. Dozov,[3] and J. P. Jolivet[4]

[1]*Laboratoire de Physique des Solides, UMR CNRS 8502, Bâtiment 510, Université Paris-Sud, 91405 Orsay, France*

[2]*European Synchrotron Radiation Facility, B.P. 220, 38043 Grenoble, France*

[3]*Nemoptic, 1 rue Guynemer, 78114 Magny-les-Hameaux, France*

[4]*Laboratoire de Chimie de la Matière Condensée, UMR CNRS 7574, Université Paris 6, 4 Place Jussieu, 75252 Paris, France*

(Received 11 October 2001; published 11 March 2002)

Aqueous suspensions of goethite (α-FeOOH) nanorods form a mineral lyotropic nematic phase that aligns in a very low magnetic field (20 mT for samples 20 μm thick). The particles orient along the field direction at intensities smaller than 350 mT, but they reorient perpendicular to the field beyond 350 mT. This outstanding behavior is also observed in the isotropic phase which has a very strong magnetic-field induced birefringence that could be interesting for applications. We interpret these magnetic effects as resulting from a competition between a nanorod remanent magnetic moment and a negative anisotropy of its magnetic susceptibility.

DOI: 10.1103/PhysRevLett.88.125507 PACS numbers: 61.30.–v, 64.70.Md, 75.50.Ee, 77.84.Nh

Recent developments in solution phase chemistry [1] have sparked renewed interest in lyotropic liquid crystalline phases formed by mineral colloidal particles [2]. Mineral liquid crystals (MLCs), of nematic, smectic, and hexagonal symmetries, formed by nanometric rods [3], ribbons [4], disks [5], and sheets [6], have been discovered and investigated from structural and thermodynamic points of view. A promising feature of MLCs is that they can combine the properties of liquid crystals (i.e., fluidity and anisotropy) with the electronic properties of mineral compounds (i.e., magnetism, conductivity, etc.). Indeed, applying a magnetic [7] or an electric [8] field to a mineral nematic phase allows one to control the orientation of assemblies of anisotropic nanoparticles by an external action. In this Letter, we consider aqueous suspensions of goethite (α-FeOOH) nanorods. Goethite is a widespread iron oxide, used mostly as pigment in the industry [9]. We show that goethite suspensions form a lyotropic nematic phase that aligns in very low magnetic fields. Moreover, the nanorods align parallel to the field at intensities below 350 mT, but reorient perpendicularly beyond. Besides, initially isotropic suspensions display a very strong field-induced anisotropy that also reverses sign at 350 mT. To the best of our knowledge, this behavior is unprecedented in the field of liquid crystals and directly results from the peculiar magnetic properties of goethite nanorods.

Suspensions of goethite nanorods were synthesized according to published procedures [10]. The *p*H of an aqueous $Fe(NO_3)_3$ solution (400 mL, 0.1 M) was raised up to 11 by adding a NaOH (1 M) solution. The resulting precipitate was aged at room temperature for 15 days, centrifuged and dispersed in a HNO_3 (3 M) solution. The suspension was again centrifuged and the solid dispersed in water, forming a *p*H 3 suspension (final volume $\approx$ 5 mL). At this *p*H, the surface charge density reaches its maximum, 0.2 C $\cdot$ m^{-2}, ensuring the suspension colloidal stability. The suspensions proved stable against sedimentation for at least a year. The ionic strength is 0.05 M in the nematic phase (NO_3^- counterions). These suspensions should not be confused with those of akaganeite (β-FeOOH) nanorods that form colloidal smectics, also called "schiller layers" [11]. The particle sizes, determined by scanning transmission electron microscopy and x-ray diffraction line broadening, are polydisperse with average length of 150 nm, width of 25 nm, and thickness of 10 nm. Actually, these dimensions may vary, depending on synthesis conditions. The volume fractions, ϕ, of the synthesis batches were determined by weight loss upon drying at 200 °C. Samples of volume fractions ranging from 2×10^{-4} to 0.085 were prepared by dilution from these initial suspensions, at constant *p*H. All samples were fluid. They were held in flat glass optical (VitroCom) capillaries of path length ranging from 20 to 100 μm.

The liquid-crystalline and magnetic properties of goethite suspensions were probed by three different techniques. Texture observations were made by polarized light microscopy. Small-angle x-ray scattering (SAXS) experiments on beam line ID2 of ESRF [12] were performed to study the nanorod orientation and to determine the nematic order parameter [13]. The magnetic birefringence of isotropic suspensions was measured by using an optical photoelastic modulator setup [14]. In each setup, the beam (x rays or light) was perpendicular to the flat plates of the capillary. The magnetic field was applied perpendicular to the beam except at ESRF where it was also applied along the x-ray beam. The magnetic induction, produced by permanent magnets or by an electromagnet, ranged between 5 and 900 mT.

The suspensions were first investigated in zero field. At high enough volume fraction, when stored vertically, they demix into a top optically isotropic (I) phase and a bottom fluid birefringent one (Fig. 1a). This simple observation proves that goethite suspensions form a lyotropic liquid crystal. The birefringent phase displays both a threaded texture and a SAXS pattern (see below and Fig. 2a) typical for nematics (N). The phase separation, with a

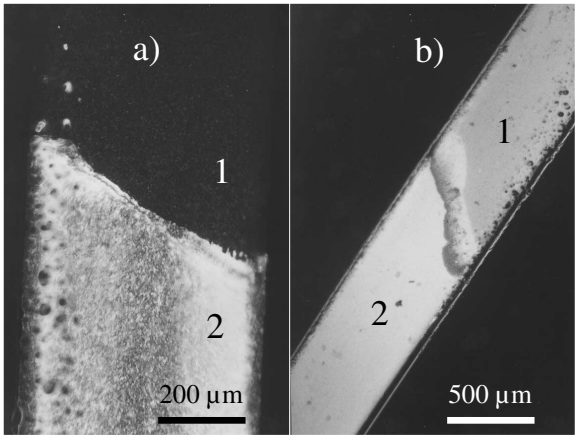

FIG. 1. Optical textures in polarized light microscopy of (a) macroscopic phase separation between the isotropic (1) and nematic (2) phases, and (b) the same sample aligned in a 20 mT vertical field, showing the paranematic (1) and nematic (2) phases.

well-defined interface, reveals a first-order phase transition. The nematic order parameter at the transition, estimated by SAXS (see below), is $S_2 = 0.9 \pm 0.1$. Heating a biphasic sample up to 100 °C had very little influence on the phase equilibrium, showing that the system can roughly be considered athermal. These last three points suggest a qualitative description of this I/N transition by the Onsager model [15]. The volume fractions of the isotropic and nematic phases at coexistence are 5.5% and 8.5%, respectively. Since the particles have a low aspect ratio, these values should be compared with simulations for hard spherocylinders [16] rather than with the Onsager model. Actually, the particles can be modeled by hard spherocylinders of a larger effective diameter reflecting the repulsion of the electrostatic double layers [17]. This leads to a transition at volume fractions $\phi \approx 15\%$, comparable to the experimental values.

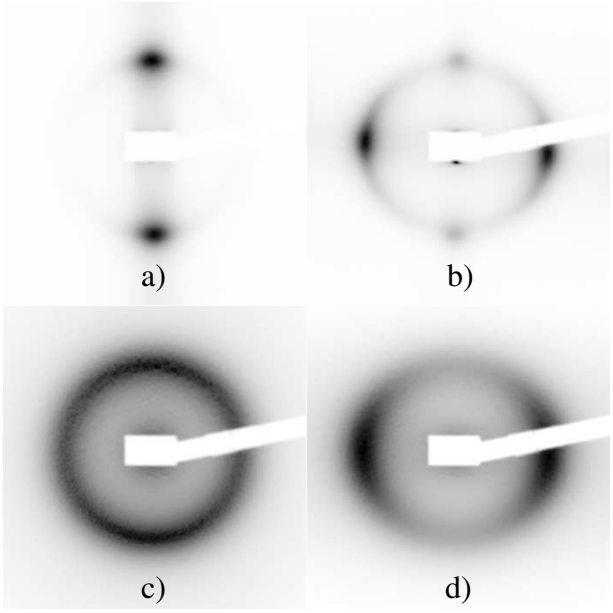

FIG. 2. SAXS patterns of (a) a nematic phase sample in a 30 mT field, (b) a nematic phase sample in a 625 mT field, (c) an isotropic phase sample in a 270 mT field, and (d) an isotropic phase sample in a 900 mT field.

A weak constant magnetic field was then applied to the nematic phase of coexistence volume fraction (8.5%). As observed by microscopy, all disclination lines vanish, the phase aligns in a few minutes along the field and forms a single domain (Fig. 1b), even in a very low magnetic field. Actually, samples held in 20 μm thick flat capillaries aligned beyond a field threshold of only 20 ± 5 mT (bend Frederiks transition) [18]. This field intensity is 50 times lower than expected for the twist Frederiks transition in the tobacco mosaic virus (TMV) [19] or in V_2O_5 suspensions 20 μm thick [7]. It is about 25 times lower than observed for usual thermotropic liquid crystals [18].

Applying a magnetic field larger than the Frederiks threshold allowed us to produce a nematic single domain. Its SAXS pattern (Fig. 2a) is typical of a lyotropic nematic phase of stiff rodlike moieties. It shows two diffuse spots located along a direction perpendicular to the director. These spots arise from the lateral interferences between nanorods and therefore indicate the particle orientation. From the position of the spots, one can derive the average distance between nanorods in the plane perpendicular to the director: $d \approx 60$ nm at $\phi = 8.5\%$. Moreover, this SAXS pattern yields a very high nematic order parameter: $S_2 = 0.9 \pm 0.1$ at 30 mT.

Strikingly, increasing the magnetic field intensity, without changing its direction, induces reorientation instabilities around 250 mT. Transient stripes, perpendicular to the field, form along the capillary. Similar stripes were observed in other lyotropic nematics like the TMV suspensions when the field direction is suddenly rotated by 90° [19]. This suggests that the goethite nanorods start rotating away from the field when its intensity reaches 250 mT. Above, the nanorods are essentially perpendicular to the magnetic field. This reorientation is clearly observed on the SAXS patterns. The nematic director, initially parallel to the magnetic field (below 250 mT), is now perpendicular to the field (Fig. 2b). To our knowledge, this is a very surprising and so far unknown behavior for a liquid crystal.

The particle reorientation around 250 mT is not specific to the nematic phase. The isotropic phase displays a strong field-induced anisotropy and its SAXS patterns show that the particles also reorient upon increasing magnetic field. For low field intensities ($B \leq 350$ mT), the particles partially align along the field (Fig. 2c). Nevertheless, experiments with the beam parallel to the field showed that the scattering is isotropic around the field direction. Thus, the angular distribution is uniaxial with preferred orientation along the field direction (the nematic order parameter tensor can be represented as a prolate ellipsoid). S_2 increases from 0 at zero field up to 0.10 ± 0.05

at 250 mT. This value is relatively large and suggests the existence of a paranematic phase [20]. At 350 mT, the scattering becomes isotropic again; the samples are then optically isotropic as well. At larger fields ($B \geq 350$ mT), the nanorods orient in the plane perpendicular to the magnetic field (Fig. 2d). The scattering remains isotropic around the field direction showing that the particle distribution concentrates towards the plane normal to the field (oblate ellipsoid). This results in a negative order parameter $S_2 = -0.25 \pm 0.01$ at 900 mT, a very high value for a paranematic phase. (Indeed, perfect order would correspond to $S_2 = -0.5$). Since the particles show orientation reversal around 350 mT in the isotropic phase as well, then this phenomenon simply reflects the individual magnetic properties of the nanorods, even though it should be enhanced by collective effects in the nematic phase.

A direct consequence of nanorod orientation in the isotropic phase is its magnetic birefringence [21]. This effect allowed us to study quantitatively the evolution of the orientation with field intensity, much more easily than in the nematic phase where the texture is heterogeneous and anchoring problems arise. The birefringence Δn of a dilute suspension of rods is given by $\Delta n = \Delta n_{\text{sat}} \phi S_2$ where Δn_{sat} is the specific birefringence of a perfectly aligned suspension. $\Delta n_{\text{sat}} = 0.80 \pm 0.03$ was measured with an optical compensator on a nematic single domain of known order parameter. The field dependence of Δn was measured for $2 \times 10^{-4} \leq \phi \leq 5.5 \times 10^{-2}$ (isotropic phase at coexistence). These curves look similar. Δn scales as B^2 at low field, reaches a maximum at 250 mT, and reverses sign at 350 mT (Fig. 3a). The curves for different volume fractions can be scaled with a ϕ-dependent factor that diverges for a volume fraction (6%) slightly above that of the isotropic phase at coexistence.

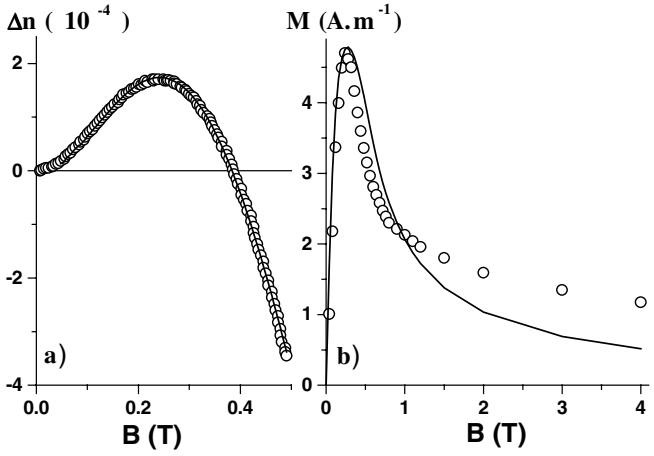

FIG. 3. (a) Magnetic birefringence of an isotropic phase sample versus magnetic field intensity (volume concentration $\phi = 3.63\%$). (b) Remanent magnetization of an isotropic sample ($\phi = 5.5\%$) frozen under field. The curves are fitted (solid lines) using the model described in the text.

This concentration effect is comparable to that observed in other lyotropics [21].

The highly unusual magnetic behavior of the suspensions was unexpected because bulk goethite is a typical antiferromagnetic material [22]. However, the magnetic properties of nanorods differ from those of bulk material, and it appears that the particles carry a small magnetic moment, possibly due to uncompensated surface spins [22]. Thus, we try to understand the magnetic behavior by the following rough argument: let us consider an assembly of identical nanorods of volume V carrying a longitudinal moment μ (neglecting polydispersity). The easy anisotropy axis lies along the particle. Since the magnetic field intensity (up to 1 T) is well below the spin-flop transition (20 T for natural goethite [22]), then the particle magnetization can be regarded as linear in field and the exchange and anisotropy energies as constant. Moreover, magnetic interactions between particles and self-demagnetizing effects are negligible. In the dilute regime, neglecting also hard-core interaction, the field-dependent part of the magnetic energy of a particle can be expressed by

$$E = -\mu B \cos\theta - \frac{V \Delta\chi B^2}{2\mu_0} \cos^2\theta , \qquad (1)$$

where θ is the angle between the nanorod axis and the external field, and $\Delta\chi = \chi_{\parallel} - \chi_{\perp}$ is the difference between the magnetic susceptibilities along and across the particle axis. The order parameter S_2 is derived as

$$S_2 = -\frac{1}{2} + \frac{1}{2J} + \frac{K^2}{6J^2} - \frac{3J\cosh K + K \sinh K}{\operatorname{erf}\left(\frac{3J-K}{\sqrt{6J}}\right) + \operatorname{erf}\left(\frac{3J+K}{\sqrt{6J}}\right)} \times \sqrt{\frac{2}{3\pi J^3}}\, e^{-(3J/2)-(K^2/6J)}, \qquad (2)$$

where erf is the error function, $J = -V\Delta\chi B^2/(3\mu_0 kT)$ and $K = \mu B/(kT)$, which finally gives $\Delta n(\phi, B)$. Figure 3a shows the fit of the experimental curve by this expression, with $\mu \approx 3 \times 10^3 \mu_B$ and $\Delta\chi \approx -5 \times 10^{-3}$ where μ_B is the Bohr magneton. (Considering polydispersity changes these values to $\mu \approx 10^3 \mu_B$ and $\Delta\chi \approx -5 \times 10^{-4}$, but does not alter the shape of the curve.) Preliminary SQUID measurements of frozen nematic suspensions have indeed shown the existence of an uncompensated moment along the particle axis.

The change of sign of Δn on Fig. 3a is due to the competition between the linear and quadratic terms in Eq. (1). The linear term induces $S_2 > 0$ at low field, while the quadratic term is responsible for the strong negative S_2 at high field. At $B = B_c$ the two terms balance, yielding $S_2 = 0$. To study in more detail the order induced by the magnetic field we expand the orientation distribution $f(\theta) = \exp(-E/kT)/\int_0^{\pi} 2\pi \sin\theta \exp(-E/kT)\, d\theta$ in Legendre polynomial series

$$f(\theta) = \sum_{n=0}^{\infty} \frac{2n+1}{4\pi} S_n P_n(\cos\theta) , \qquad (3)$$

where $S_n = \langle P_n(\cos\theta)\rangle$ is the order parameter of rank n. By symmetry, only even values of n are allowed in a usual nematic phase [18]. However, in the "paranematic" phase considered here, the potential in Eq. (1) gives a strong contribution to the odd rank order parameters. On Fig. 3b we present S_1 (multiplied by μ and the particle number density) as a function of B, calculated from Eq. (3). For $B \approx B_c$ the vectorial (or polar) order parameter S_1 is very high. At $B > B_c$, S_1 decreases, but remains nonnegligible even at very high fields. The phase is then approximately paranematic, but with negative S_2 (i.e., oblate order tensor), and some residual polar order. In between these two regimes, the competition between the positive S_1 and the negative S_2 gives a very particular ordering, never predicted nor observed experimentally; the system is uniaxial, but $f(\theta)$ has a maximum for some $\theta = \theta_m$, with $0 < \theta_m < \pi/2$. The particles are then oriented preferentially on a revolution cone with field-dependent aperture θ_m. At $B = B_c$, $S_2 = 0$, the birefringence and all other second order tensor properties vanish (θ_m is close to the "magic" angle). However, the phase is not isotropic, because all the S_n with $n \neq 2$ remain finite. These predicted features, mainly due to the linear term in Eq. (1) can be directly tested experimentally, e.g., from the macroscopic anisotropy of vector (dipolar) properties. We performed SQUID measurements of the remanent (in zero field) magnetic moment of an isotropic suspension ($\phi = 5.5\%$) previously frozen under field. This moment is proportional to $\langle \mu \cos\theta\rangle$. The experimental curve (Fig. 3b) corresponds qualitatively to the results of the model for the vectorial order parameter S_1. This curve also yields the average particle magnetic moment $\mu \approx 2 \times 10^3 \mu_B$ which has the same order of magnitude as the value used to fit the birefringence.

In conclusion, liquid-crystalline phases based on mineral nanoparticles can display very unexpected physical properties. This is nicely illustrated by the competition between dipolar and quadrupolar orders that govern the magnetic behavior of goethite suspensions. Other original effects are likely to be observed in liquid-crystalline suspensions of carefully selected mineral moieties.

We are deeply indebted to J. Hernandez for drawing our attention to this experimental system, to H. Lekkerkerker and L. Fruchter for helpful discussions, and to J. C. P. Gabriel, F. Camerel, C. Bourgaux, and J. Chavanne for help during the synchrotron experiments at LURE and ESRF.

*Electronic address: davidson@lps.u-psud.fr

[1] J. P. Jolivet, *Metal Oxide Chemistry and Synthesis; From Solution to Solid State* (Wiley, Chichester, U.K., 2000).
[2] For a recent review, see, J. C. P. Gabriel and P. Davidson, Adv. Mater. **12**, 9 (2000).
[3] M. P. B. van Bruggen, F. M. van der Kooij, and H. N. W. Lekkerkerker, J. Phys. Condens. Matter **8**, 9451 (1996), and references therein.
[4] P. Davidson *et al.,* J. Phys. II (France) **5**, 1577 (1995).
[5] A. B. D. Brown, C. Ferrero, T. Narayanan, and A. R. Rennie, Eur. Phys. J. B **11**, 481 (1999); F. M. van der Kooij, K. Kassapidou and H. N. W. Lekkerkerker, Nature (London) **406**, 868 (2000).
[6] J. C. P. Gabriel *et al.,* Nature (London) **413**, 504 (2001).
[7] X. Commeinhes, P. Davidson, C. Bourgaux, and J. Livage, Adv. Mater. **9**, 900 (1997).
[8] S. Lamarque-Forget *et al.,* Adv. Mater. **12**, 1267 (2000).
[9] R. M. Cornell and U. Schwertmann, *The Iron Oxides* (VCH, Weinheim, Germany, 1996).
[10] R. J. Atkinson, A. M. Posner, and J. P. Quirk, J. Phys. Chem. **71**, 550 (1967).
[11] H. Zocher and W. Heller, Z. Anorg. Allg. Chem. **186**, 75 (1930); H. Maeda and Y. Maeda, Langmuir **12**, 1446 (1996).
[12] P. Boesecke, O. Diat, and B. Rasmussen, Rev. Sci. Instrum. **66**, 1636 (1995).
[13] P. Davidson, D. Petermann, and A. M. Levelut, J. Phys. II (France) **5**, 113 (1995).
[14] E. Hasmonay *et al.,* Eur. Phys. J. B **5**, 859 (1998).
[15] L. Onsager, Ann. N.Y. Acad. Sci. **51**, 627 (1949).
[16] P. Bolhuis and D. Frenkel, J. Chem. Phys. **106**, 666 (1997).
[17] G. J. Vroege and H. N. W. Lekkerkerker, Rep. Prog. Phys. **55**, 1241 (1992).
[18] P. G. de Gennes and J. Prost, *The Physics of Liquid Crystals* (Clarendon, Oxford, U.K., 1995).
[19] S. Fraden *et al.,* J. Phys. (Paris), Colloq. **46**, 85 (1985).
[20] I. Lelidis and G. Durand, Phys. Rev. E **48**, 3822 (1993), and references therein.
[21] S. Fraden, G. Maret, and D. L. D. Caspar, Phys. Rev. E **48**, 2816 (1993).
[22] J. M. D. Coey *et al.,* J. Phys. Condens. Matter **7**, 759 (1995).